Adsorption 3, 107–115 (1997)

Comparison of Molecular Simulation of Adsorption with Experiment

ALAN L. MYERS
Department of Chemical Engineering, University of Pennsylvania, Philadelphia, PA, 19104, USA

JOSE A. CALLES AND GUILLERMO CALLEJA
Department of Chemical Engineering, Universidad Complutense, Madrid, 28040, Spain

Received September 19, 1996; Revised October 1, 1996; Accepted October 4, 1996

Abstract. Experimental measurements of adsorption yield the surface excess. The Gibbs surface excess is the actual or absolute amount of gas contained in the pores less the amount of gas that would be present in the pores in the absence of gas-solid intermolecular forces. Molecular simulation of adsorption yields the absolute amount adsorbed. Comparison of simulated adsorption isotherms and heats of adsorption with experiment requires a conversion from absolute to excess variables. Molecular simulations of adsorption of methane in slit pores at room temperature show large differences between absolute and excess adsorption. The difference between absolute and excess adsorption may be ignored when the pore volume of the adsorbent is negligible compared to the adsorption second virial coefficient ($V \ll B_{1s}$).

Keywords: adsorption, molecular simulation, isosteric heat

1. Introduction

Computer simulations of adsorption yield the statistical average of the number of molecules in the pores of the adsorbent, called absolute adsorption. Experiments yield the surface excess (Sircar, 1985), which is the number of molecules in the pores (absolute adsorption) minus the number that would be present in the pore without adsorption at the density of the bulk gas. Similarly, the energy measured in experiments is the excess energy, which is the actual energy of the molecules in the pores minus the energy of adsorbate gas occupying non-adsorbing pores of the same volume. The most important variables are the amount adsorbed (adsorption isotherm) and isosteric heat of adsorption.

Experimental data are reported, sometimes explicitly but more often implicitly, in terms of excess variables: excess amount adsorbed, excess enthalpy, excess isosteric heat, etc. The standard experimental procedure for measurement of adsorption isotherms is the volumetric method. The excess amount adsorbed is obtained directly from a mass balance: the total amount of gas introduced to the sample cell minus the amount in the gas phase. The amount in the gas phase is calculated from the equilibrium values of temperature and pressure, the dead space in the sample cell, and the equation of state for the bulk gas. The dead space, which includes the pore volume of the adsorbent, is calculated from the perfect-gas law by adding helium at low pressure and room temperature to the evacuated sample cell containing the adsorbent.

Molecular simulation of adsorption is based upon a model of the microporous structure of the adsorbent. The simulation box includes the solid and the micropores in which adsorption occurs. For zeolites, the simulation box is composed of one or more unit cells. Molecular simulation of adsorption yields the absolute amount of gas in the pores and the total energy of gas-gas and gas-solid interactions. The conversion of absolute adsorption obtained by molecular simulation to excess adsorption for comparison with experiment

has been discussed previously (Karavias and Myers, 1991; Nicholson, 1996), but we are unaware of any systematic comparisons of absolute and excess adsorption isotherms. This paper also covers the conversion of the absolute heat of adsorption obtained from molecular simulation to the excess heat of adsorption obtained from calorimetry.

The subject of this paper is the conversion of absolute variables obtained by molecular simulation to excess variables for comparison with experiment. The system chosen for study is methane adsorbed between slits of graphite at room temperature. The slit size and potential parameters for the simulation were chosen to mimic adsorption of methane in carbon with a specific surface area of 870 m^2/g. However, in this work, the accuracy of the molecular model is less important than comparing absolute adsorption to excess adsorption.

2. Absolute and Excess Variables for Adsorption

Thermodynamic Properties of Bulk Gas Phase

For the range of pressures in this study, the properties of the gas phase are described by the virial equation of state terminated after the second virial coefficient:

$$z = \frac{Pv}{kT} = 1 + \frac{B_{11}P}{kT} \tag{1}$$

For this equation of state, the fugacity is related to the pressure by:

$$f = P \exp\left(\frac{B_{11}P}{kT}\right) \tag{2}$$

The residual enthalpy (Smith et al., 1996) of the gas phase is:

$$h^R = (h - h^\circ) = (B_{11} - B'_{11}T)P \tag{3}$$

and the residual internal energy of the gas phase is:

$$u^R = (u - u^\circ) = -B'_{11}TP \tag{4}$$

where $B'_{11} = dB_{11}/dT$. u° and h° are the internal energy and enthalpy, respectively, in the perfect-gas state at the temperature of the simulation.

Absolute Variables

Absolute adsorption refers to the actual number of molecules (N^a) in the simulation box. The absolute isosteric heat is (Karavias and Myers, 1991; Nicholson and Parsonage, 1982):

$$q^a_{st} = h^R + kT - \bar{u}^a \tag{5}$$

Residual enthalpy h^R is calculated (for this work) from Eq. (3). The differential enthalpy in the adsorbed phase is given by:

$$\bar{u}^a = \frac{dU^a}{dN^a} \tag{6}$$

The reference state for U^a is the perfect-gas state at the temperature of the simulation.

Excess Variables

The simulations yield absolute quantities: the absolute number of molecules in the simulation box (N^a) and the absolute value of the total potential energy of gas-gas and gas-solid interactions (U^a). Experimental data obtained by standard volumetric or gravimetric methods are excess quantities (Sircar, 1985). The excess amount adsorbed N^e is:

$$N^e = N^a - V\rho^b \tag{7}$$

where ρ^b is the bulk density calculated from an equation of state:

$$\rho^b = \frac{P}{zkT} \tag{8}$$

and $z = PV/kT$ is the compressibility factor in the bulk gas phase.

V is the pore volume of the adsorbent. Experimentally, the value of V is determined from volumetric measurements using helium at room temperature and low pressure under the reasonable assumption that the adsorption of helium is negligible. In the case of idealized geometries like a slit, the geometric volume may be calculated from the surface area and slit width. For complicated pore structures like zeolites, V may be determined from the perfect-gas law by molecular simulation of "adsorption" of helium atoms in the pores at low pressure and at 300 K. Determination of the dead-space volume of the pores using helium atoms is consistent with experiment.

The excess energy of adsorption (U^e) is:

$$U^e = U^a - V\rho^b u^R \tag{9}$$

The excess isosteric heat is given by Eq. (5) with absolute energy replaced by excess energy:

$$q_{st}^e = h^R + kT - \bar{u}^e \tag{10}$$

In terms of excess variables, the differential internal energy in the adsorbed phase is given by:

$$\bar{u}^e = \frac{dU^e}{dN^e} \tag{11}$$

Conversion from Absolute to Excess Variables

Grand-canonical Monte Carlo (GCMC) simulation of adsorption yields the absolute adsorption N^a and the absolute energy of adsorption U^a (relative to the perfect-gas state) as ensemble averages. The independent variables are the temperature and the chemical potential, which is converted to a pressure by the equation of state.

Conversion of absolute (N^a) to excess (N^e) adsorption by Eq. (7) is straightforward. The pore volume (V) for the simulation should be determined by modeling helium atoms at low pressure and room temperature, since this is the experimental method for measuring the dead space in the sample cell.

The absolute isosteric heat is obtained from Eq. (5) by numerical differentiation of the function $U^a(N^a)$ along an isotherm. Alternatively, $\bar{u}^a$ may be obtained directly from fluctuations (Nicholson and Parsonage, 1982) in N^a and U^a by:

$$\bar{u}^a = \frac{f(U^a, N^a)}{f(N^a, N^a)} \tag{12}$$

where the notation $f(X, Y) = \langle XY\rangle - \langle X\rangle\langle Y\rangle$ refers to the co-variance of X-Y pairs.

Since the quantities subtracted from the absolute variables to obtain the excess variables in Eqs. (7) and (9) are constants, fluctuations cannot be used to calculate the excess isosteric heat. The excess isosteric heat needed for comparison with experiment is obtained from Eq. (10) by differentiation of the function $U^e(N^e)$ at constant temperature, or by applying the Clapeyron equation to the function $P(T)$ at constant excess adsorption.

3. Molecular Model and Simulation Procedure

Gas-Solid Interaction Potential

Carbon micropores were modeled as slits between walls composed of triply stacked planes of graphite. Lateral variations in the gas-solid potential were smoothed by integration in the xy-plane to yield the 10–4 potential of Steele (1974):

$$U_{1s}(z) = 2\pi\rho_s\sigma_{1s}^2\epsilon_{1s}\left[\frac{2}{5}\left(\frac{\sigma_{1s}}{z}\right)^{10} - \sum_{i=0}^{2}\left(\frac{\sigma_{1s}}{z+id}\right)^4\right] \tag{13}$$

where z is the distance from the adsorbate molecule to the nearest plane in the stack. $d = 0.334$ nm is the distance between basal planes of graphite; $\rho_s = 38.2$ atom/nm^2 is the area density of carbon atoms in the basal plane of graphite; σ_{1s} and ϵ_{1s} are the gas-solid potential parameters for the interaction of an adsorbate molecule with a single carbon atom. Equation (13) is for one wall of the slit; the total potential energy U_{1s}^t for one adsorbate molecule inside a slit pore of width H is the sum of the interactions with both walls:

$$U_{1s}^t(z) = U_{1s}(z) + U_{1s}(H - z) \tag{14}$$

where H is the distance between the graphite planes (center-to-center distance between carbon atoms) forming the walls of the slit. Additivity of intermolecular forces was assumed for both gas-gas and gas-solid interactions.

The surface area of microporous slits separated by three basal planes of graphite is 870 m^2/g.

Gas-Gas Interaction Potential

Adsorbate-adsorbate interactions were modeled with the Lennard-Jones 12–6 potential:

$$U_{11}(r) = 4\epsilon_{11}\left[\left(\frac{\sigma_{11}}{r}\right)^{12} - \left(\frac{\sigma_{11}}{r}\right)^6\right] \tag{15}$$

where r is the distance between molecular centers. The potential parameters from Steele (1974) are listed in Table 1; parameters for the gas-solid interaction were estimated with Lorentz-Berthelot mixing rules:

$$\begin{aligned}\sigma_{ij} &= \frac{1}{2}(\sigma_{ii} + \sigma_{jj}) \\ \epsilon_{ij} &= (\epsilon_{ii}\cdot\epsilon_{jj})^{0.5}\end{aligned} \tag{16}$$

Table 1. Potential parameters used in the simulations.

Pair	σ, nm	ϵ/k, K
CH_4-CH_4	0.382	148.2
C-C	0.340	28.0
C-CH_4	0.361	64.4

Table 2. Second virial coefficients for methane.

T, K	B_{11}, cm^3/mol	B'_{11}, cm^3/(mol-K)
270	−55.4	0.480
300	−42.8	0.376
330	−32.6	0.301

Simulation Method

Monte Carlo simulations of adsorption were performed in the grand canonical ensemble (Allen and Tildesley, 1987; Dunne et al., 1996; Karavias and Myers, 1991; Matranga et al., 1992; Nicholson and Parsonage, 1982), for which independent variables are the temperature, volume, and chemical potential. The grand-canonical Monte Carlo (GCMC) method generates a Markov chain of configurations. Values for the equilibrium energy and number of molecules adsorbed are determined by averaging the values generated by the Markov chain. The chemical potential (μ) of the adsorbate is related to its fugacity (f) by:

$$f = \frac{kT}{\Lambda^3} \exp\left(\frac{\mu}{kT}\right) \tag{17}$$

where $\Lambda = h/\sqrt{2\pi mkT}$ is the thermal de Broglie wavelength; h is Planck's constant and m is the mass of the molecule.

The molecular simulations were performed within a rectangular box of volume L^2H bounded on the top and bottom by walls composed of triply stacked basal planes of graphite. The total surface area of the graphite basal planes forming the top and bottom of the box was $2L^2$. In dimensionless terms, $L^* = L/\sigma_{11} = 10$ and simulations were performed for $H^* = H/\sigma_{11} = 3, 4, 5, 6$, and 7. The minimum image convention (Allen and Tildesley, 1987) and a cutoff distance $r_c = 2.5\sigma_{11}$ was used with periodic boundary conditions in the x and y directions. Interactions of adsorbate molecules with adsorbate molecules in neighboring slits were neglected. The GCMC cycle of moving a molecule chosen randomly, attempting to create a new molecule at a position chosen randomly, and attempting to destroy a molecule chosen randomly was performed. The magnitude of attempted displacements was tuned periodically for an acceptance probability of one-half.

The pore volume of the slit was calculated from:

$$V = L^2(H - \sigma_{cc}) \tag{18}$$

with $\sigma_{cc} = 0.340$ nm. The slit width was decreased by one-half the diameter of a carbon atom on each side to account for the presence of the carbon atoms. The value of V from Eq. (18) agreed within 2% with the value obtained from the perfect-gas law by molecular simulation of "adsorption" of helium atoms at low pressure and 300 K. Since the value of the pore volume V is used to correct absolute adsorption to excess adsorption, and since the correction term normally does not exceed 10%, an error of 2% in V corresponds to an error of only 0.2% in the amount adsorbed. Nevertheless, for comparison with experimental data, the preferred method for calculating V is the molecular simulation of helium "adsorption."

Runs of 1.5×10^6 cycles were required for convergence to equilibrium values of the total number of molecules N^a in the simulation box and the total potential energy U^a. The estimated uncertainty in the values of N^a and U^a is less than 2%.

Values of B_{11} and B'_{11} in Table 2 for the properties of bulk methane gas were calculated from the tables of Hirschfelder et al. (1954) using the potential parameters in Table 1.

Absorption was expressed in specific terms (mol/kg) by:

$$n^a = \frac{N^a}{3L^2\rho_s A_c} \tag{19}$$

where $A_c = 12.01$ = atomic weight of carbon.

4. Results

Adsorption isotherms at 300 K for excess adsorption calculated from Eq. (7) are plotted on Fig. 1 for slit widths ranging from $H^* = 3$ to $H^* = 7$. The specific adsorption is highest at $H^* = 3$ because the

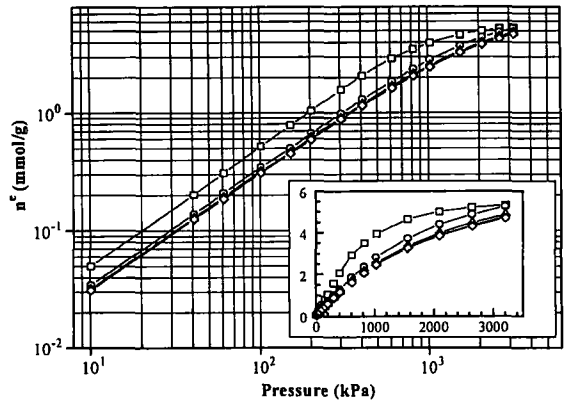

Figure 1. Adsorption isotherms as a function of slit width at 300 K. Amount adsorbed is surface excess. (□): $H^* = 3$; (○): $H^* = 4$; (△): $H^* = 5$; (▽): $H^* = 6$; (◇): $H^* = 7$.

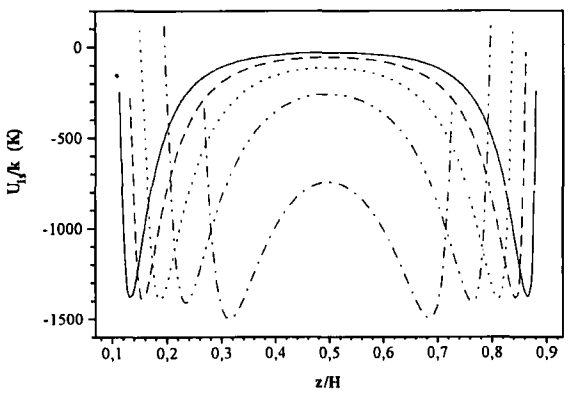

Figure 2. Methane-carbon potential energy along z axis for different slit widths. (———): $H^* = 7$; (— — —): $H^* = 6$; (- - - - -): $H^* = 5$; (— - - —): $H^* = 4$; (— - —): $H^* = 3$.

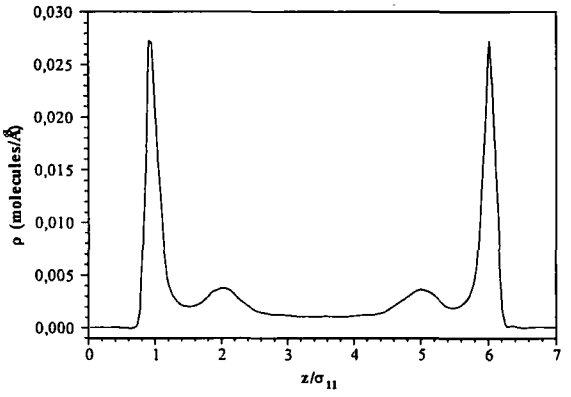

Figure 3. Profile of methane density in slit along z axis perpendicular to basal planes of graphite at 300 K and 3.2 MPa. Slit width $H^* = 7$.

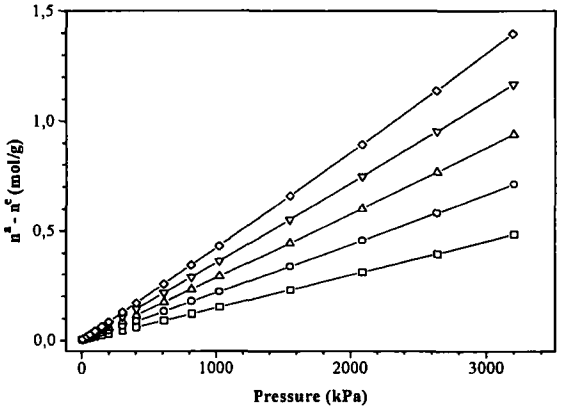

Figure 4. Difference between absolute and excess loading at 300 K for different slit widths. (□): $H^* = 3$; (○): $H^* = 4$; (△): $H^* = 5$; (▽): $H^* = 6$; (◇): $H^* = 7$.

gas-solid potentials from walls on opposite sides of the slit overlap. This overlap effect is illustrated by the plot of Eq. (14) shown on Fig. 2 for different slit widths. For $H^* = 3$, the potential energy of adsorption $U_{1s}/k = -750$ K at the center of the slit. For $H^* = 7$, the adsorptive potential at the center of the slit is close to zero. The excess adsorption is the same for slit widths $H^* > 4$ because most of the adsorbed molecules are confined to single layers close to the top and bottom of the slit. Figure 3 shows the density profile for a slit width $H^* = 7$ at 3.2 MPa and 300 K. The formation of a second layer is evident, but at the center of the slit the density approaches that of the bulk gas phase.

The difference between excess adsorption and absolute absorption is shown on Fig. 4 for slit widths ranging from $H^* = 3$ to $H^* = 7$. The difference between the absolute and excess adsorption is directly proportional to the pore volume, which for the slit model is proportional to the slit width. The difference between absolute and excess adsorption is also proportional to the pressure. It is interesting that the limiting slopes dN^e/dP and dN^a/dP are unequal at the limit of zero pressure. Even for the smallest slit width $H^* = 3$, which corresponds to a distance of $3\sigma_{11} = 1.145$ nm and is just wide enough to accommodate two adsorbed layers of methane molecules, the ratio N^a/N^e is 1.03 at the limit of zero pressure.

The difference between the absolute and excess values for isosteric heat are shown in Fig. 5 for slit widths (H^*) ranging from 3 to 7. For adsorption on a smoothed graphitic plane, the heat of adsorption is expected to

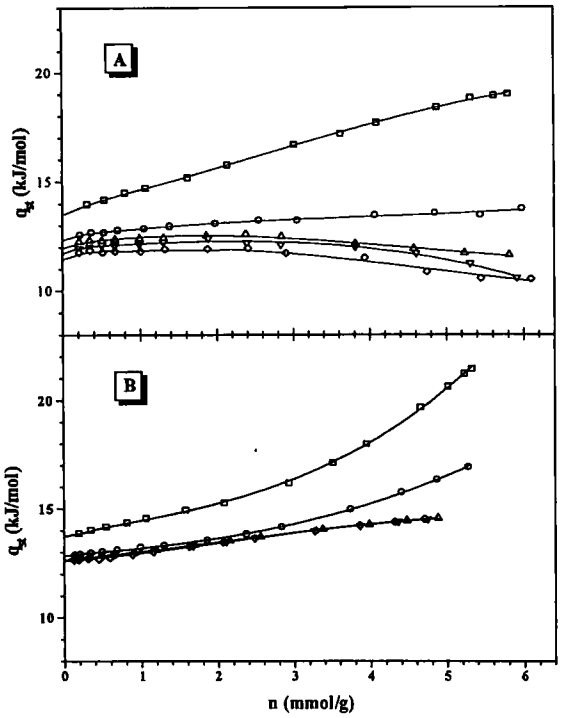

Figure 5. Isosteric heats of adsorption at 300 K for different slit widths: (A) Absolute isosteric heat versus absolute loading; (B) Excess isosteric heat versus excess loading. (□): $H^* = 3$; (○): $H^* = 4$; (△): $H^* = 5$; (▽): $H^* = 6$; (◇): $H^* = 7$.

increase with coverage as a result of cooperative interactions between adsorbed molecules. The expected cooperative effect is observed for the excess isosteric heat q_{st}^e. However, the absolute isosteric heat of adsorption q_{st}^a decreases with loading for $H^* > 4$, an effect usually associated with energetic heterogeneity of gas-solid interactions. In this case, the surface of minimum potential energy is perfectly smooth. The absolute energy of adsorption per molecule decreases with coverage because every molecule inside the slit is counted as adsorbed. Another feature of Fig. 5 is that the absolute isosteric heat decreases with pore size, but the excess isosteric heat is independent of the pore volume for $H^* > 4$.

The excess and isosteric heats of adsorption are compared in Fig. 6 for a slit width of $H^* = 7$. It is interesting that the absolute and excess isosteric heats are different even at the limit of zero coverage. The absolute and excess isosteric heats are related by:

$$q_{st}^a = q_{st}^e \left(\frac{d\bar{U}^a/dP}{d\bar{U}^e/dP}\right)\left(\frac{dn^e/dP}{dn^a/dP}\right) \tag{20}$$

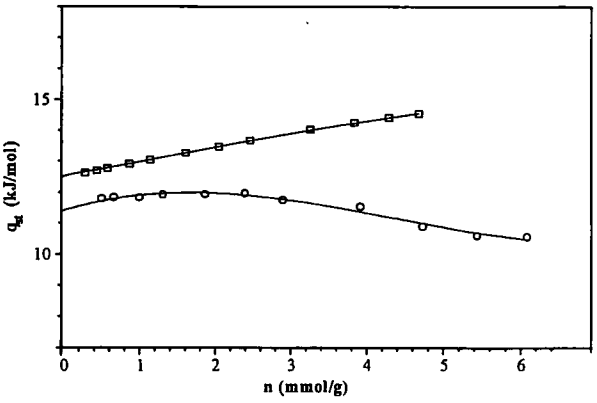

Figure 6. Isosteric heats of methane absorption at 300 K for slit width $H^* = 7$. (□): excess heat q_{st}^e; (○): absolute heat q_{st}^a.

At the limit of zero coverage, the slope $(d\bar{U}^a/dP)/(d\bar{U}^e/dP)$ is unity but the slope $(dn^e/dP)/(dn^a/dP)$ is less than unity. Therefore at the limit of zero coverage, the absolute isosteric heat is smaller than the excess isosteric heat. The difference $(q_{st}^a - q_{st}^e)$ increases from 10% at the limit of zero coverage of 25% at a coverage of 4 mmol/g. The excess heat of adsorption shows the cooperative effect associated with non-heterogeneous surfaces, but the profile of the absolute heat of adsorption incorrectly suggests the presence of energetic heterogeneity in the gas-solid interaction energies.

Limits at Zero Coverage

In terms of excess variables, the limiting slope of the absorption isotherm at zero pressure is given by the adsorption second virial coefficient B_{1s}^e:

$$\lim_{P\to 0} N^e = \frac{B_{1s}^e P}{kT} \tag{21}$$

where

$$B_{1s}^e = \int [e^{-U/kT} - 1]\, dV \tag{22}$$

The integral is over the pore volume V of the adsorbent. At the limit of zero pressure $U^a = U^e = U$.

Similarly for absolute variables, the limiting slope of the adsorption isotherm at the limit of zero pressure is:

$$\lim_{P\to 0} N^a = \frac{B_{1s}^a P}{kT} \tag{23}$$

Table 3. Adsorption second virial coefficients (B_{1s}) and isosteric heats of adsorption (q_{st}°) for CH_4 in carbon slits at limit of zero coverage as a function of slit width $H^* = H/\sigma_{11}$. $T = 300$ K.

Slit width H^*	B_{1s}, cm^3/g		q_{st}, kJ/mol	
	Absolute	Excess	Absolute	Excess
3	12.73	12.38	13.39	13.70
4	9.16	8.63	12.26	12.83
5	8.72	8.03	11.88	12.67
6	8.71	7.85	11.64	12.61
7	8.80	7.78	11.44	12.59

where

$$B_{1s}^{a} = \int e^{-U/kT}\, dV \tag{24}$$

The isosteric heat of adsorption at the limit of zero coverage is given by (Valenzuela and Myers, 1989):

$$q_{st} = k\left[\frac{d \ln B_{1s}}{d(1/T)}\right] + kT \tag{25}$$

Therefore:

$$q_{st}^{e} = \frac{\int[(-U)e^{-U/kT}]\, dV}{\int[e^{-U/kT} - 1]\, dV} \tag{26}$$

and

$$q_{st}^{a} = \frac{\int[(-U)e^{-U/kT}]\, dV}{\int e^{-U/kT}\, dV} \tag{27}$$

Adsorption second virial coefficients and isosteric heats of adsorption calculated from Eqs. (22), (24), (26), and (27) are given in Table 3.

Comparison of Eqs. (22) and (24) shows that the difference between the second virial coefficients for excess and absolute adsorption is the pore volume of the adsorbent (V). For example, for a pore width $H^* = 5$, the pore volume of the adsorbent is about 0.7 cm^3/g. Therefore, the difference between absolute and excess adsorption can be neglected when the pore volume is negligible compared to the adsorption second virial coefficient. In this case, the pore volume is about 9% of the adsorption second virial coefficient, so the correction from absolute to excess adsorption in necessary. At low temperature where $B_{1s} \gg V$, the difference between absolute and excess adsorption is negligible.

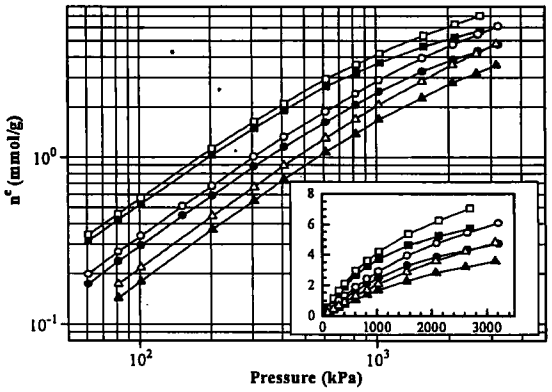

Figure 7. Adsorption isotherms at different temperatures for slit width $H^* = 7$. Open symbols are absolute values and solid symbols are excess values. (□): 270 K; (○): 300 K; (△): 330 K.

Comparison with Clapeyron Equation

An alternative to Eqs. (5) and (10) for the isosteric heat of adsorption is the Clapeyron equation (Karavias and Myers, 1991):

$$q_{st} = -k\left(\frac{\partial \ln f}{\partial(1/T)}\right)_{n} + h^{R} \tag{28}$$

Holding the excess adsorption constant gives the excess isosteric heat:

$$q_{st}^{e} = -k\left(\frac{\partial \ln f}{\partial(1/T)}\right)_{n^e} + h^{R} \tag{29}$$

Holding the absolute adsorption constant gives the absolute isosteric heat:

$$q_{st}^{a} = -k\left(\frac{\partial \ln f}{\partial(1/T)}\right)_{n^a} + h^{R} \tag{30}$$

Absolute and excess adsorption isotherms at 270, 300, and 330 K are shown on Fig. 7 for $H^* = 7$. Heats of adsorption calculated from the adsorption isotherms on Fig. 7 by means of Eqs. (29) and (30) agree with the results plotted on Fig. 6; the excellent agreement (average error 2%) is a verification of the internal consistency of the simulation data.

5. Conclusions

The difference between absolute and excess adsorption depends upon the system and the temperature. The magnitude of the difference increases with pore size and temperature.

The difference between absolute and excess adsorption may be ignored when the pore volume of the adsorbent is negligible compared to the adsorption second virial coefficient ($V \ll B_{1s}$). For example, for adsorption on NaX at room temperature (Dunne et al., 1996), the adsorption second virial coefficients of O_2 and CO_2 are 2.6 and 21,000 cm^3/g, respectively. The pore volume of NaX is approximately 0.2 cm^3/g; therefore, the difference between absolute and excess adsorption is large for O_2 but negligible for CO_2. Adsorptive separations are performed most frequently at a temperature where some components are strongly adsorbed and other components are weakly adsorbed. In most cases, the difference between absolute and excess adsorption is large for the weakly adsorbed species (e.g., O_2 in separation of air using zeolites).

For the system studied in this work, CH_4 in carbon at room temperature, the adsorption second virial coefficient was $\approx$10 cm^3/g. Henry's constants for absolute adsorption are larger than those for excess adsorption; differences range from 3% for a pore volume of 0.35 cm^3/g to 13% for a pore volume of 1.02 cm^3/g. The difference between absolute and excess adsorption increases with loading up to 3 MPa, where the difference is 10–25% depending upon the pore volume. The excess heat of adsorption is larger than the absolute heat. At the limit of zero coverage, differences between excess and absolute heats of adsorption range from 2% for a pore volume of 0.35 cm^3/g to 10% for a pore volume of 1.02 cm^3/g. The magnitude of the difference between absolute and excess adsorption increases with loading.

Nomenclature

B_{11} second virial coefficient in bulk gas phase
B'_{11} dB_{11}/dT
B_{1s} adsorption second virial coefficient
d spacing of basal planes of graphite
f fugacity
H slit width
H^* dimensionless slit width H/σ_{11}
h° enthalpy in perfect gas state
h^R residual enthalpy in bulk gas phase, Eq. (3)
k Boltzmann constant
L length of one side of simulation box
L^* dimensionless length L/σ_{11}
N number of adsorbed molecules
n specific adsorption, mol/kg
P pressure
q_{st} isosteric heat of adsorption
r distance between centers of molecules
T temperature
U energy
U_{11} gas-gas interaction energy
U_{1s} gas-solid interaction energy
u° internal energy in perfect gas state
u^R residual internal energy in bulk gas phase, Eq. (4)
$\bar{u}$ differential energy (dU/dN) in adsorbed phase
V pore volume of adsorbent
v molar volume
z compressibility factor, Eq. (1); distance from graphite plane, Eq. (13)

Greek Letters

ϵ_{11} potential parameter for energy of methane-methane interaction, Eq. (15)
ϵ_{1s} potential parameter for energy of carbon-methane interaction, Eq. (13)
λ thermal de Broglie wavelength, Eq. (17)
μ chemical potential
ρ^b density in bulk gas phase
ρ_s area density of carbon atoms in basal plane of graphite
σ_{11} collision diameter for methane-methane interaction, Eq. (15)
σ_{1s} collision diameter for carbon-methane interaction, Eq. (13)

Superscripts

a refers to absolute variables
e refers to excess variables

Acknowledgments

This research was supported by a grant (NSF CTS 9213832) from the National Science Foundation.

References

Allen, M.P. and D.J. Tildesley, *Computer Simulation of Liquids*, Oxford Univ. Press, Oxford, 1987.

Dunne, J.A., A.L. Myers, and D.A. Kofke, "Simulation of Adsorption of Liquid Mixtures of N_2 and O_2 in a Model Faujasite Cavity at 77.5 K," *Adsorption*, **2**, 41–50 (1996).

Dunne, J.A., M. Rao, S. Sircar, R.J. Gorte, and A.L. Myers, "Calorimetric Heats of Adsorption and Adsorption Isotherms. II. O_2, N_2,

Ar, CO_2, CH_4, C_2H_6, and SF_6 on NaX, H-ZSM-5, and Na-ZSM-5 Zeolites," *Langmuir*, 1996, in press.

Hirschfelder, J.O., C.F. Curtiss, and R.B. Bird, *Molecular Theory of Gases and Liquids*, p. 1114, John Wiley & Sons, Inc., New York, 1954.

Karavias, F. and A.L. Myers, "Monte Carlo Simulations of Adsorption of Non-Polar and Polar Molecules in Zeolite X," *Molec. Sim.*, **8**, 23–50 (1991).

Karavias, F. and A.L. Myers, "Isosteric Heats of Multicomponent Adsorption: Thermodynamics and Computer Simulations," *Langmuir*, **7**, 3118–3126 (1991).

Matranga, K., A.L. Myers, and E.D. Glandt, "Storage of Natural Gas by Adsorption on Activated Carbon," *Chem. Eng. Science*, **47**, 1569–1579 (1992).

Nicholson, D. and N.G. Parsonage, *Computer Simulation and the Statistical Mechanics of Adsorption*, Academic Press, NY, 1982.

Nicholson, D., "Using Computer Simulation to Study the Properties of Molecules in Micropores," *J. Chem. Soc., Faraday Trans.*, **92**, 1–9 (1996).

Sircar, S., "Excess Properties and Column Dynamics of Multicomponent Gas Adsorption," *J. Chem. Soc., Faraday Trans. I*, **81**, 1541–1545 (1985).

Smith, J.M., H.C. Van Ness, and M.M. Abbott, *Introduction to Chemical Engineering Thermodynamics*, 5th Ed., p. 472, McGraw-Hill, NY, 1996.

Steele, W.A., *The Interaction of Gases with Solid Surfaces*, Pergamon Press, Oxford, 1974.

Valenzuela, D. and A.L. Myers, *Adsorption Equilibrium Data Handbook*, Prentice-Hall, Englewood Cliffs, NJ, 1989.